

## Supporting material

### *Zerovalent iron nanoparticles-alginate nanocomposites for Cr(VI) removal in water. Influence of temperature, pH, dissolved oxygen, matrix and nZVI surface composition*

Marguerite Parnis<sup>a,b</sup>, Fabiana Elena García<sup>a,c</sup>, Melanie Toledo<sup>c</sup>, Víctor Nahuel Montesinos<sup>\*a,c</sup> and Natalia Quici<sup>a,c</sup>

<sup>a.</sup> División Química de la Remediación Ambiental, Centro Atómico Constituyentes, CNEA, CONICET, Gral. Paz 1499, San Martín Buenos Aires, Argentina.

<sup>b.</sup> École Nationale Supérieure de Chimie de Montpellier, Montpellier, France

<sup>c.</sup> Centro de Tecnologías Químicas, Departamento de Ingeniería Química, FRBA-UTN, Buenos Aires, Argentina.

#### Physicochemical characteristics of both commercial nZVI

**Table S1.** Main characteristics of NSTAR and N25 nanoparticles informed by the provider, Nanoiron s.r.o.<sup>1</sup>.

	Composition	Size (nm)	S.S.A. (m <sup>2</sup> g <sup>-1</sup> )	Oxide layer thickness
<b>NSTAR</b>	Fe(0) ≥ 65-80% Fe <sub>3</sub> O <sub>4</sub> ≤ 20-35%	50-65	20-25	4.8 <sup>2</sup>
<b>N25</b>	Fe(0) = 80-85% Fe <sub>3</sub> O <sub>4</sub> = 15-20%	40-65	25	1.8 <sup>3*</sup>

\*Thickness of N25 iron oxide layer reference was taken from Ribas “25P” nanoparticles given that the manufacturer indicates that N25 is the slurry version of N25P. It is noteworthy to say that the oxide layer might change over time due to aging effect that inially can activate the nanoparticles, blurring the oxide layer limits.

### Effect of the sonication procedure in the removal efficiency

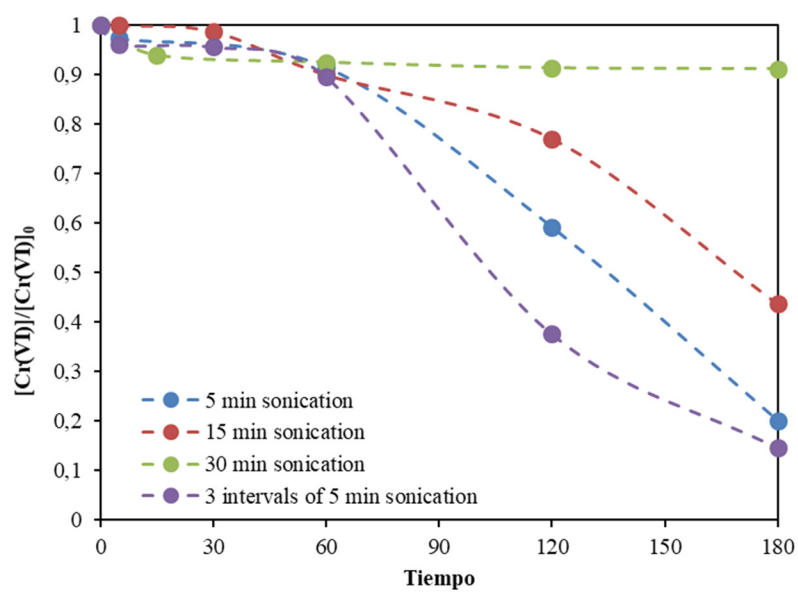


Figure S1. Relative Cr(VI) removal for different sonication protocols.

## SEM-EDS. Mapping and backscattered electrons of nZVI@AL

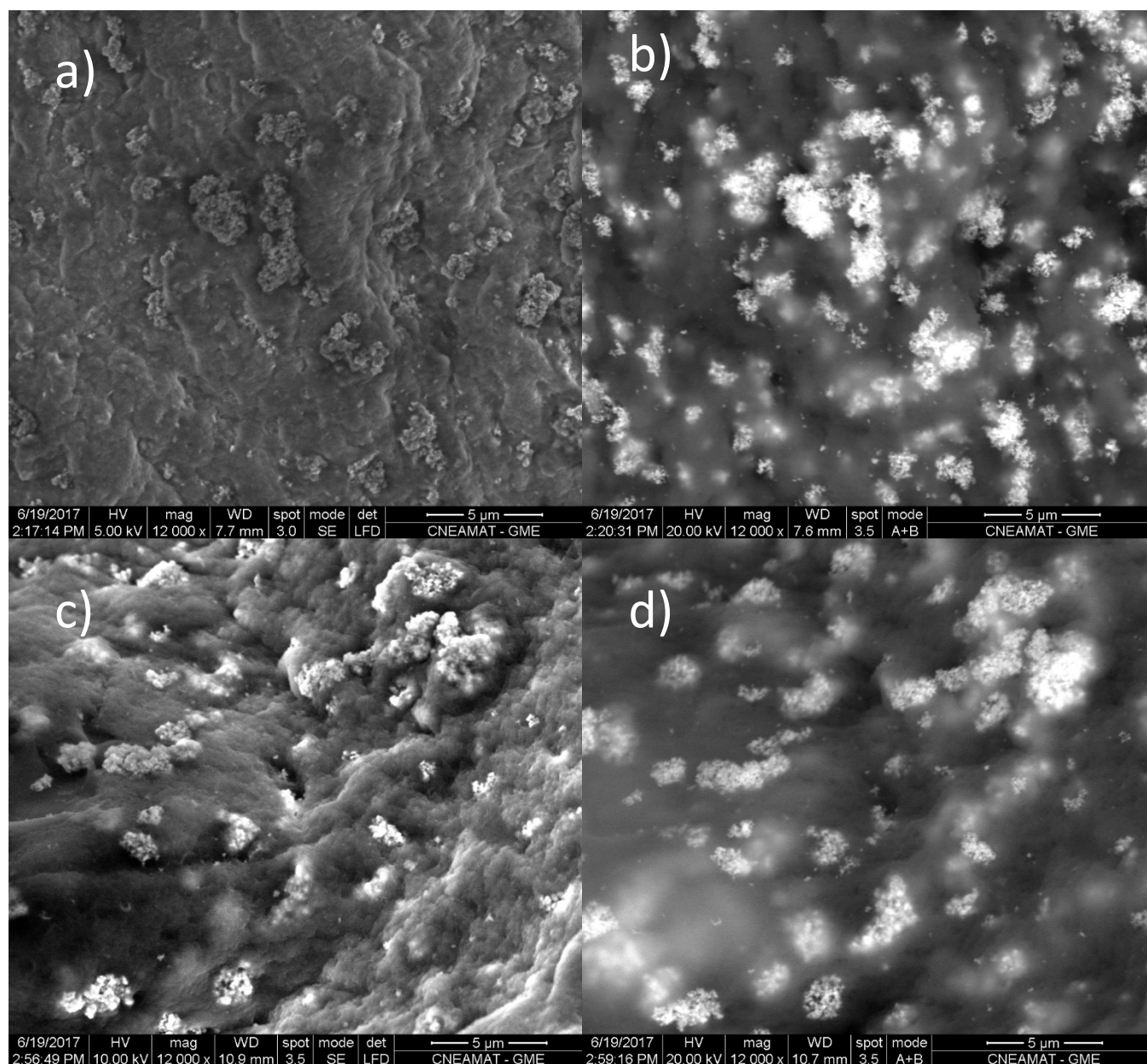
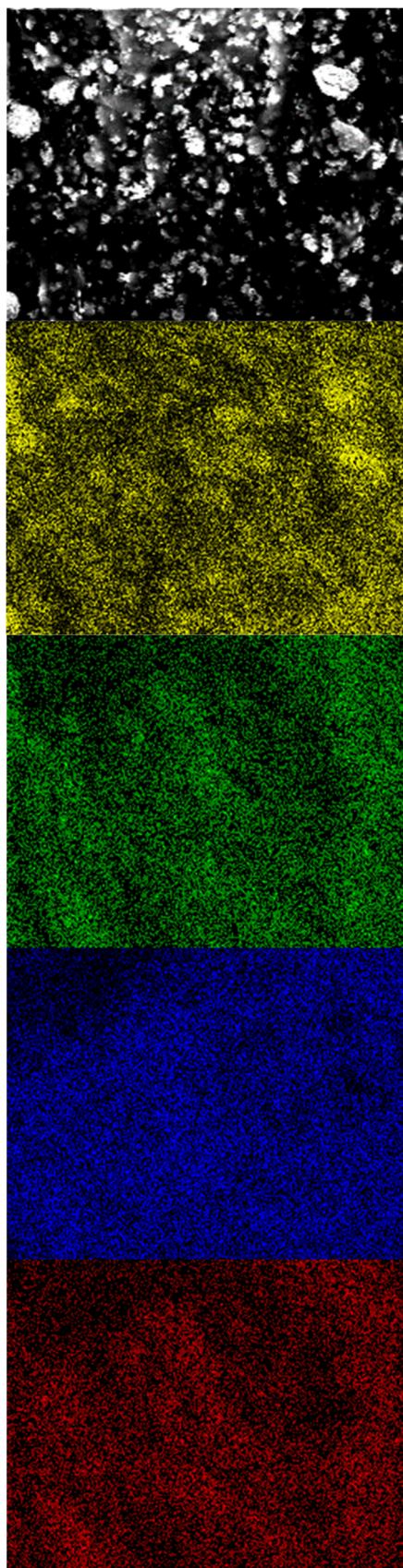


Figure S2. Secondary electrons SEM image for a) N25@AL and c) NSTAR@AL. Backscattered electrons SEM image for c) N25@AL and d) NSTAR@AL.

Secondary electrons increased the contrast between electrons coming from Fe atoms with respect to lighter elements as Ca, C, O and H that constitute the backbone of the polymeric matrix.



SE-SEM

FeK

OK

CaK

CK

Figure S3. EDS Mapping of NSTAR@AL bead.

# Proportion of iron released after synthesis of nZVI@AL beads

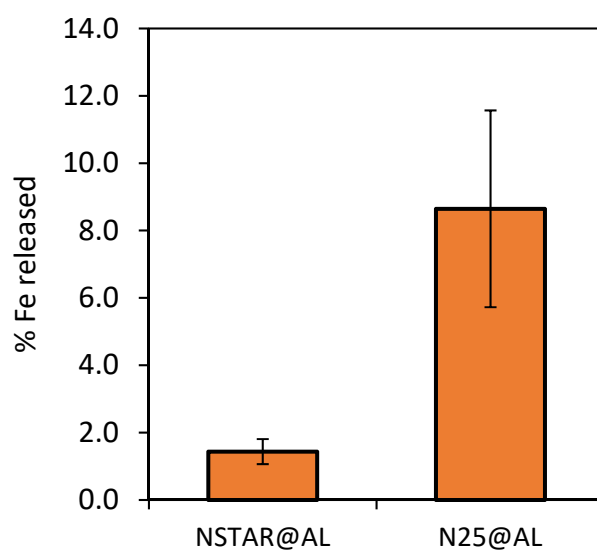


Figure S4. Percentual iron delivered into the solution  $\text{CaCl}_2$  solution after nZVI immobilization. Each bar correspond to the results obtained after the synthesis of four batches of each type of bead.

# Effect of Alginate viscosity in the removal efficiency

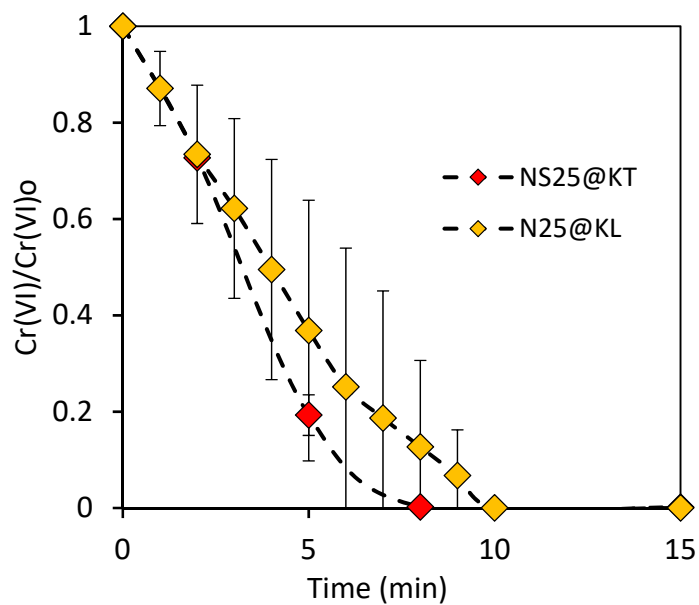


Figure S5. Effect of d) alginate viscosity in Cr(VI) removal by N25@AL.  $[\text{Cr(VI)}]_0 = 64 \mu\text{M}$ ,  $n\text{ZVI@AL} = 1 \text{ g}$ ,  $\text{MR (Fe:Cr)} = 55$

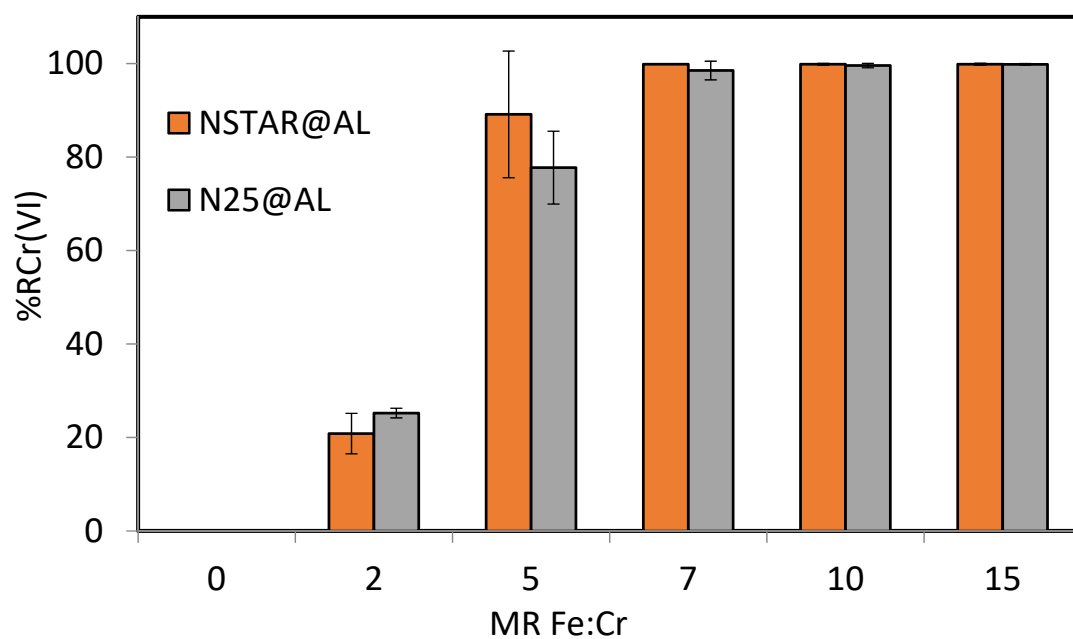


Figure S6. Maximum removal capacity of N25@AL and NSTAR@AL. nZVI@AL = 1 g, pH 3, T = 25 °C.